

SHORT COMMUNICATIONS

Acta Cryst. (1996). **A52**, 497–498

Comment on Contrast of HOLZ lines in energy-filtered convergent-beam electron diffraction patterns from silicon by Lehmpfuhl, Krahl & Uchida (1995)

L. J. ALLEN* AND T. W. JOSEFSSON *at School of Physics, University of Melbourne, Parkville, Victoria 3052, Australia. E-mail: lja@physics.unimelb.edu.au*

(Received 13 January 1996; accepted 19 January 1996)

Abstract

Whilst investigating higher-order Laue-zone (HOLZ) lines in convergent-beam electron diffraction (CBED) patterns for silicon near low-indexed zone axes, Lehmpfuhl, Krahl & Uchida [*Acta Cryst.* (1995), **A51**, 504–514] concluded that there is a strong anisotropy in the Debye–Waller factor at room temperature. It is demonstrated here that no such anisotropy is implied by their experimental results.

Lehmpfuhl, Krahl & Uchida (1995) have taken convergent-beam electron diffraction (CBED) patterns for the zero beam near the [111], [100] and [110] zone axes of silicon at a nominal electron energy of 100 keV and for a range of temperatures. At room temperature, they were able to filter out electrons that had undergone energy losses of greater than 2 eV. This filtering enhanced the contrast of the higher-order Laue-zone (HOLZ) lines in the CBED zone-axis patterns. They compared their experimental results with simulations of the CBED patterns using the Bloch-wave formulation of dynamical electron diffraction theory. Absorption was included in the simulations using the expression (Voss, Lehmpfuhl & Smith, 1980)

$$V_{g_{im}} = V_{g_{real}}(Ag - Bg^2) \quad (1)$$

for small scattering angles, where g^2 is the sum of squares of the reflection indices. For larger scattering angles, as is the case for reflections from the first-order Laue zone (FOLZ), they used the following expression due to Ichimiya & Lehmpfuhl (1978):

$$V_{g_{im}} = C \exp(-Fg^2) \{\text{lattice factor}\}. \quad (2)$$

The quantities A , B , C and F are constants.

Using this model for absorption, which is mainly due to thermal diffuse scattering (TDS), and a Debye–Waller factor $\exp(-Ds^2)$ with $D = 0.46 \text{ \AA}^2$ (Aldred & Hart, 1973), Lehmpfuhl, Krahl & Uchida (1995) found disagreement between the intensity of the HOLZ lines in their simulated zero-order CBED patterns and those measured experimentally at room temperature. For the [111] zone axis, they found that best agreement could be obtained for an adjusted value of $D = 0.26 \text{ \AA}^2$. For the [100] pattern, the HOLZ lines in the simulation showed a maximum accompanied by two minima – see Fig. 5(c) in Lehmpfuhl, Krahl & Uchida (1995) – in disagreement with the experiment. Only by reducing the Debye–Waller factor to $D = 0.13 \text{ \AA}^2$ were they able to obtain reasonable agreement between experiment and theory in this case, suggesting a strong anisotropy in the Debye–Waller factor at this temperature. It will be sufficient for the purposes of this communication to focus on these two cases.

We have simulated the energy-filtered room-temperature [111] and [100] CBED patterns using the formulation of the dynamical Bloch-wave theory given by Allen & Rossouw (1989), which allows the HOLZ beams to be easily and accurately incorporated in the calculation. The absorptive part of the potential is calculated using the Einstein model (Hall & Hirsch, 1965; Allen & Rossouw, 1990; Bird & King, 1990). Absorption needed to be included exactly rather than perturbatively when solving the scattering equations (Allen & Rossouw, 1989) to obtain agreement with the experimental results. To ensure accurate atomic structure factors for large scattering angles and hence accurate absorptive potentials in the Einstein model (particularly pertinent to the HOLZ beams), we have used the recent parametrizations for X-ray scattering factors of Waasmeier & Kirfel (1995) but less accurate parametrizations (Doyle & Turner, 1968; Rez, Rez & Grant, 1994) gave similar results.

In Fig. 1, we show the zero-order CBED disc calculated with $D = 0.46 \text{ \AA}^2$ for the [111] zone axis for a nominal voltage of 100 kV. An energy of 99.177 keV, corresponding to a wavelength of 0.03718 Å, was used in the simulation, the same as used by Lehmpfuhl, Krahl & Uchida (1995). The thickness of the sample was assumed to be 2200 Å. 88 beams were used in the simulation, 27 in the FOLZ. The result can be compared with Fig. 1(a) of Lehmpfuhl, Krahl & Uchida (1995). The fine detail indicated by the three arrows shown on their experimental result are all well reproduced by the simulation.

Fig. 2 shows a simulation of the zero-order CBED disc for the [100] zone axis. Once again, the energy is 99.177 keV. The sample thickness is 2720 Å. 93 beams were used (48 in the

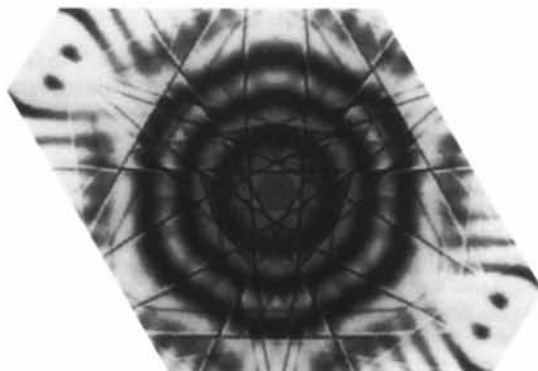


Fig. 1. Zero beam of CBED pattern near [111] zone axis showing FOLZ lines. The wavelength is 0.03718 Å and the thickness is 2200 Å. 88 beams were used and absorption included using the Einstein model, $D = 0.46 \text{ \AA}^2$.

FOLZ). This is in good agreement with Fig. 5(a) of Lehmpfuhl, Krahl & Uchida (1995). The anomalous behaviour in the HOLZ-line intensities for $D = 0.46 \text{ \AA}^2$ found by Lehmpfuhl, Krahl & Uchida (1995) is not present.

The value of $D = 0.46 \text{ \AA}^2$ (Aldred & Hart, 1973) used in the simulations is consistent with other experimental evidence (Butt & Bashir, 1988) and gave excellent agreement with the experimental zero-order CBED patterns for both [111] and

[100] zone axes when the Einstein model was used to represent the absorption due to TDS (provided that this is not included perturbatively). Therefore, our calculations suggest that no anisotropy in the Debye–Waller factor should be concluded from the experimental results of Lehmpfuhl, Krahl & Uchida (1995). This is consistent with theoretical expectations that, for silicon at room temperature, anharmonic contributions to the Debye–Waller factor should be small (Sears & Shelley, 1991).

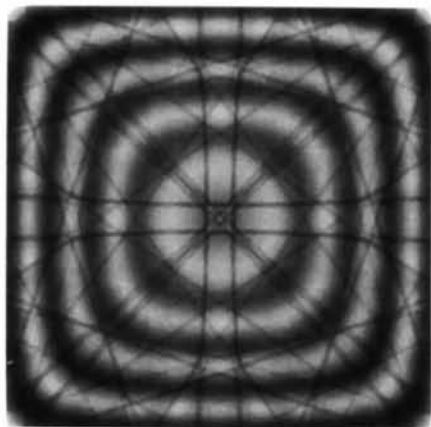


Fig. 2. Zero beam of CBED pattern near [100] zone axis showing FOLZ lines. The wavelength is 0.03718 \AA and the thickness 2720 \AA . 93 beams were used and absorption included using the Einstein model, $D = 0.46 \text{ \AA}^2$.

References

- Aldred, P. J. & Hart, M. (1973) *Proc. R. Soc. London Ser. A*, **332**, 223–254.
 Allen, L. J. & Rossouw, C. J. (1989). *Phys. Rev. B*, **39**, 8313–8321.
 Allen, L. J. & Rossouw, C. J. (1990). *Phys. Rev. B*, **42**, 11644–11654.
 Bird, D. M. & King, Q. A. (1990). *Acta Cryst. A* **46**, 202–208.
 Butt, N. M. & Bashir, J. (1988). *Acta Cryst. A* **44**, 396–398.
 Doyle, P. A. & Turner, P. S. (1968). *Acta Cryst. A* **24**, 390–397.
 Hall, C. R. & Hirsch, P. B. (1965). *Proc. R. Soc. London Ser. A*, **286**, 158–177.
 Ichimiya, A. & Lehmpfuhl, G. (1978). *Z. Naturforsch. Teil A*, **33**, 269–281.
 Lehmpfuhl, G., Krahl, D. & Uchida, Y. (1995). *Acta Cryst. A* **51**, 504–514.
 Rez, D., Rez, P. & Grant, I. (1994). *Acta Cryst. A* **50**, 481–497.
 Sears, V. F. & Shelley, S. A. (1991). *Acta Cryst. A* **47**, 441–446.
 Voss, R., Lehmpfuhl, G. & Smith, P. J. (1980). *Z. Naturforsch. Teil A*, **35**, 973–984.
 Waasmeier, D. & Kirfel, A. (1995). *Acta Cryst. A* **51**, 416–431.

Acta Cryst. (1996). **A52**, 498–499

X-ray topography of a lysozyme crystal

V. STOJANOFF* AND D. P. SIDONS at NSLS, Brookhaven National Laboratory, Upton, New York 11973, USA. E-mail: vstojan@bnlarm.bnl.gov

(Received 1 August 1995; accepted 2 January 1996)

Abstract

X-ray topography methods were employed to identify defects in lysozyme crystals. White-beam and monochromatic topographs of lysozyme crystals obtained at the National Synchrotron Light Source are presented.

X-ray topography is a well established technique to characterize growth- or process-induced defects. Introduced in the late 40's and early 50's by Guinier & Tennevin (1949) and by Schultz (1954), X-ray topography as we know it today derives from the techniques developed by Lang (1958), Bond & Andrus (1952) and Bonse & Kappler (1958). A review of the theoretical background and the experimental techniques for X-ray topography was presented by Tanner (1976). With the advent of synchrotron-radiation sources, X-ray topography became largely employed in material characterization. The work by Tuomi, Naukarinen & Rabe (1974) and Hart (1975) reflects

the initial stage of the application of X-ray topography to the study of as-grown or process-induced defects in materials. The purpose of the present report is to show that X-ray topography can be a valuable tool in the study and understanding of protein growth conditions and diffraction properties.

White and monochromatic synchrotron radiation from beam line X26C at the National Synchrotron Light Source (NSLS) at Brookhaven National Laboratory were employed in X-ray topographic studies of defects in protein crystals. The X26C port was 20 m from the bending magnet and the spot size at the sample was 1 mm^2 . For white-beam X-ray topography, the sample-to-film distance was of the order of 50 cm with an average exposure time of 30 s. The distance was chosen in order to avoid spot overlaps, however, the geometric resolution was decreased. In monochromatic synchrotron X-ray topography studies, a channel-cut (111) silicon crystal was employed. The crystal-to-film distance was about 10 cm and the exposures took several minutes. The geometrical resolution with the